

# Carbazole Aminoalcohols Induce Antiproliferation and Apoptosis of Human Tumor Cells by Inhibiting Topoisomerase I

Weisi Wang<sup>+, [a, c]</sup> Xiao Sun<sup>+, [b]</sup> Deheng Sun,<sup>[b]</sup> Shizhu Li,<sup>[a]</sup> Yang Yu,<sup>[b]</sup> Tingyuan Yang,<sup>[b]</sup> Junmin Yao,<sup>[a]</sup> Zhuo Chen,<sup>\*, [b]</sup> and Liping Duan<sup>\*, [a]</sup>

Novel carbazole aminoalcohols were designed and synthesized as anticancer agents. Among them, alkylamine-chain-substituted compounds showed the most promising antiproliferative activity, with IC<sub>50</sub> values in the single-digit micromolar range against two human tumor cell lines. Topoisomerase I (topo I) is likely to be one of the targets of these compounds. Results of comet assays and molecular docking indicate that the repre-

sentative compounds may act as topo I poisons, causing single-strand DNA damage by stabilizing the topo I–DNA cleavage complex. In particular, the most potent compound, 1-(butylamino)-3-(3,6-dichloro-9H-carbazol-9-yl)propan-2-ol (**6**), was shown to be able to induce G<sub>2</sub>-phase cell-cycle arrest and apoptosis in HeLa cells.

## Introduction

Eukaryotic topoisomerase I (topo I) was first discovered by Champoux and Dulbecco in 1972.<sup>[1]</sup> Topo I is able to relax supercoiled DNA and plays an essential role in DNA replication and transcription.<sup>[2,3]</sup> Topo I inhibitors are divided into two categories: topo I poisons and catalytic inhibitors. Topo I poisons stabilize the topo I–DNA cleavage complex and lead to the accumulation of DNA damage. In terms of chemical structure, most of topo I poisons share a common feature: a planar aromatic scaffold and an amine side chain (Figure 1).

Camptothecin (CPT), extracted from *Camptotheca acuminata*, is a classic topo I poison, which binds to the topo I–DNA cleavage complex and stabilizes it, thereby inducing DNA damage.<sup>[4,5]</sup> At present, CPT analogues irinotecan and topotecan are first-line anticancer drugs, which are widely used for treating small-cell lung cancer and advanced cervical cancer.<sup>[6]</sup> However, CPT analogues have well-known limitations, including chemical instability, dose-limiting side effects, and drug resistance.<sup>[6,7]</sup> Thus, the discovery of novel topo I inhibitors with dis-

tinct scaffolds is an attractive drug development strategy for tumor treatment.<sup>[8–10]</sup>

Carbazole is a prominent core structure found in numerous natural and synthetic compounds with a wide range of biological activities, including antimalarial, antineoplastic, and neuroprotective effects.<sup>[11–13]</sup> In view of anticancer agents, many carbazole derivatives have been shown to exhibit antitumor activity by targeting diverse enzymes or kinases.<sup>[14–16]</sup> However, few studies have addressed the relationships between topo I and carbazoles.<sup>[17]</sup> More generally for carbazole compounds, carbazole aminoalcohols have been reported as potential antimalarial agents<sup>[18]</sup> and neurological regulators,<sup>[19]</sup> while their antitumor capacity is unknown.

In this study, a series of carbazole aminoalcohol derivatives were designed and synthesized. Their cytotoxicity against two human cancer cell lines was evaluated. Additionally, because carbazole aminoalcohols possess the common structural feature of topo I poisons, it is reasonable to hypothesize that topo I is one of the targets of carbazole aminoalcohols. Accordingly, the topo I inhibitory activity of target compounds was also evaluated, and structure–activity relationships (SARs) are discussed herein. Comet assays and molecular docking analyses were used to predict the potential mode of action of these compounds. Furthermore, apoptosis and cell-cycle analyses were performed to reveal the antitumor mechanisms of the most potent compounds.

## Results and Discussion

### Chemistry

The synthetic routes of carbazole aminoalcohol derivatives are summarized in Scheme 1. Reaction of carbazole (**1a–c**) and epoxy chloropropane in the presence of KOH afforded the

[a] Dr. W. Wang,<sup>+</sup> Dr. S. Li, J. Yao, Dr. L. Duan  
National Institute of Parasitic Diseases, Chinese Center for Disease Control and Prevention, WHO Collaborating Centre for Malaria, Schistosomiasis, and Filariasis, Key Laboratory of Parasitology and Vector Biology of the Chinese Ministry of Health, Shanghai 200025 (China)  
E-mail: duanlp1@chinacdc.cn

[b] X. Sun,<sup>+</sup> D. Sun, Y. Yu, T. Yang, Dr. Z. Chen  
Shanghai Key Laboratory of New Drug Design, School of Pharmacy, East China University of Science and Technology, Shanghai 200237 (China)  
E-mail: chenzhuo@ecust.edu.cn

[c] Dr. W. Wang<sup>+</sup>  
ZJU-ENS Joint Laboratory of Medicinal Chemistry, College of Pharmaceutical Sciences, Zhejiang University, Hangzhou 310058 (China)

[†] These authors contributed equally to this work.

Supporting information for this article can be found under <http://dx.doi.org/10.1002/cmdc.201600391>.

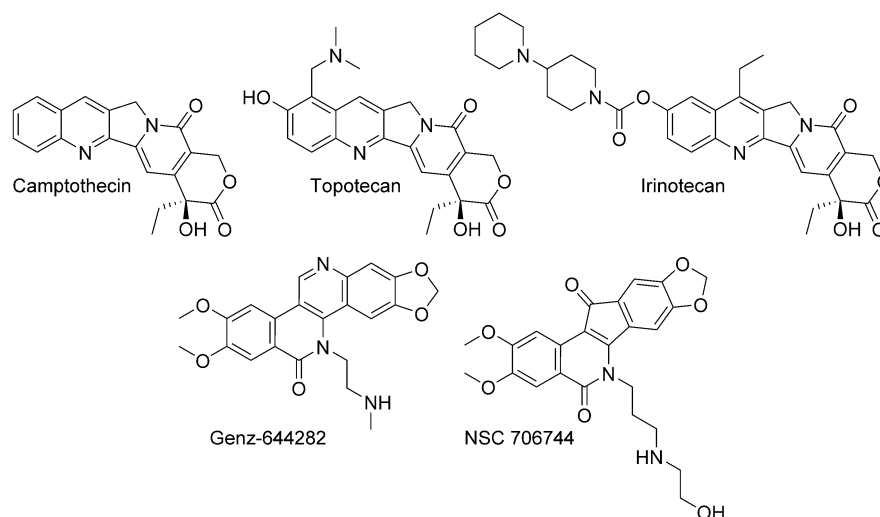
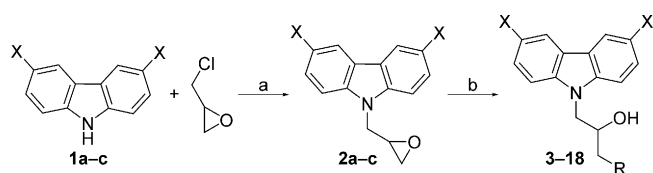


Figure 1. Structures of topo I poisons.



Scheme 1. Synthetic routes for target compounds 3–18. Reagents and conditions: a) KOH, DMF, 0 °C, 3 h; b) amines (RNH<sub>2</sub> or RR'NH), BiCl<sub>3</sub>, EtOH, reflux, 6 h, 50–71 % (over two steps).

epoxy propane intermediates **2a–c**, which subsequently reacted with appropriate amines to obtain the corresponding target compounds **3–18**.

### In vitro cytotoxicity

All the synthesized compounds were evaluated for their cytotoxicity against two human cancer cell lines: HeLa (human cervical carcinoma) and HL60 (human promyelocytic leukemia). The results are summarized in Table 1. In general, all test compounds exhibited moderate cytotoxicity, with IC<sub>50</sub> values in the micromolar range. The derivatives with aliphatic amino and benzylamino groups (**3–7**, and **15–18**) were slightly more potent than those possessing aromatic amino groups (**8–14**) in both cell lines. Among them, alkylamine tails (in **5–7**) were found to be the preferred substituents for cytotoxicity. *n*-Butylamino-substituted compound **6** exhibited the best cytotoxicity against HeLa and HL60 cells (IC<sub>50</sub>: 3.64 ± 0.65 and 4.58 ± 0.54 μM, respectively). In addition, by varying the X-group substituents of the carbazole core, we found the dichlorinated carbazole to act as a privileged core structure. Eliminating the chlorine atoms (in **17**) or replacing them with bromine atoms (in **18**) resulted in a two- to three-fold decrease in potency, respectively.

### Topo I inhibition

Taking into account the structural similarity between carbazole aminoalcohols and known topo I poisons, we theorized that the former could serve as a class of topo I inhibitors. To test this hypothesis, topo I-mediated DNA relaxation assays were performed to examine their topo I inhibitory activity. CPT was used as the reference compound.

In the preliminary assay (Figure 2A), compounds with alkylamine tails (**5–7**) displayed significant topo I inhibitory activity

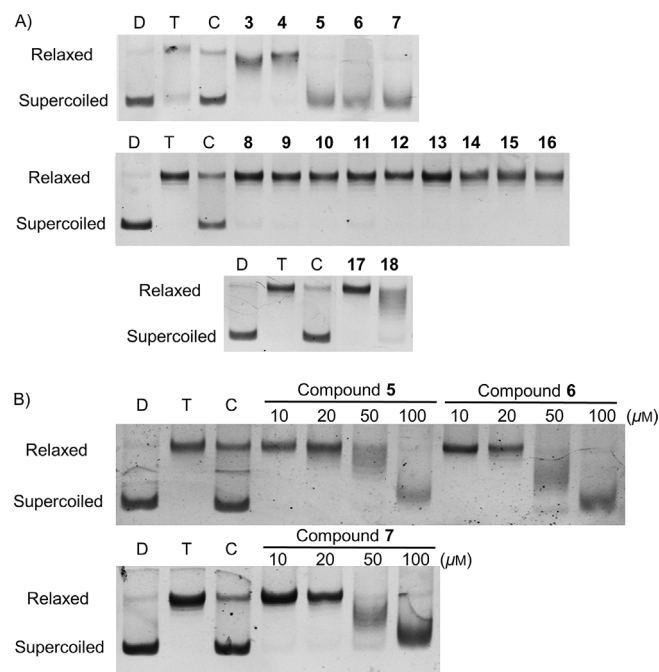


Figure 2. Inhibition of topo I-mediated DNA (pBR322) relaxation by carbazole aminoalcohols (see Experimental Section for details). D = pBR322, T = pBR322 + topo I, C = pBR322 + topo I + CPT. A) Compounds **3–18** and CPT were incubated with topo I and pBR322 at 100 μM. B) Compounds **5**, **6**, and **7** were incubated with topo I and pBR322 at concentrations of 10, 20, 50, and 100 μM.

**Table 1.** In vitro cytotoxicity of carbazole aminoalcohols 3–18.

| Compd | X  | R | IC <sub>50</sub> [μM] <sup>[a]</sup> |               |
|-------|----|---|--------------------------------------|---------------|
|       |    |   | HeLa                                 | HL60          |
|       |    |   |                                      |               |
| 3     | Cl |   | 8.73 ± 2.92                          | 9.16 ± 1.69   |
| 4     | Cl |   | 7.54 ± 1.03                          | 10.22 ± 3.39  |
| 5     | Cl |   | 9.13 ± 3.91                          | 8.87 ± 3.48   |
| 6     | Cl |   | 3.64 ± 0.65                          | 4.58 ± 0.54   |
| 7     | Cl |   | 6.43 ± 1.61                          | 5.48 ± 2.09   |
| 8     | Cl |   | 27.20 ± 7.48                         | 15.00 ± 7.91  |
| 9     | Cl |   | 25.37 ± 4.78                         | 16.11 ± 1.76  |
| 10    | Cl |   | 15.58 ± 4.04                         | 13.58 ± 3.70  |
| 11    | Cl |   | 25.86 ± 1.59                         | 19.51 ± 1.15  |
| 12    | Cl |   | 27.76 ± 3.65                         | 16.92 ± 3.01  |
| 13    | Cl |   | 32.21 ± 4.97                         | 13.60 ± 3.34  |
| 14    | Cl |   | 22.03 ± 4.21                         | 14.64 ± 6.20  |
| 15    | Cl |   | 10.41 ± 1.54                         | 10.04 ± 2.55  |
| 16    | Cl |   | 8.27 ± 1.01                          | 7.15 ± 3.12   |
| 17    | H  |   | 10.30 ± 1.43                         | 11.10 ± 4.49  |
| 18    | Br |   | 9.84 ± 4.94                          | 10.08 ± 3.48  |
| CPT   | -  | - | NT <sup>[b]</sup>                    | 0.020 ± 0.003 |

[a] Data are then mean ± SD of three independent experiments. [b] Not tested.

at a concentration of 100 μM, which were more effective than CPT. In addition, compounds 3, 4, and 18 exhibited high inhibitory activity as evidenced by their IC<sub>50</sub> values in the low micromolar range. These results are in agreement with the tendency of antiproliferative activity. In contrast, the derivatives with aromatic amino substituents (8–14) did not achieve satisfactory performance in topo I inhibition studies, and this result is also in accordance with their relatively weak cytotoxicity. It seems that steric effects and the basicity of the nitrogen atom of the amine tail affect potency, especially for topo I inhibitory activity. The use of small or flexible groups rather than bulky substituents as amino tails was beneficial for activity. Introducing more basic amino tails also had a positive effect on potency. Further investigation revealed that compounds 5–7 inhibit topo I in a dose-dependent manner (Figure 2B). In particular, at a concentration of 50 μM, all three compounds exhibited more potent topo I inhibitory ability than CPT (100 μM).

### DNA damage in HeLa cells

Inhibition of topo I, especially drug trapping of the topo I–DNA cleavage complex (like topo I poisons), frequently results in DNA damage, which triggers cell death. We therefore used comet assays to examine whether compounds 5–7 could induce an accumulation of DNA damage in HeLa cells. According to the results (Figure 3A), relative to negative control samples, a significant increase in DNA damage was observed in HeLa cells after treatment with 5–7 and CPT at a concentration of 10 μM. Tail DNA reveals the actual DNA damage. The greater percentage of DNA in the tail implies more DNA damage.<sup>[20]</sup> Notably, the olive tail moments of compounds 6 and 7 were 34.9 and 39.8%, respectively, about two-fold more than the extent induced by CPT (18.7%, Figure 3B). The results indicated that, in HeLa cells, compounds 6 and 7 cause DNA damage more efficiently than CPT under the same conditions.

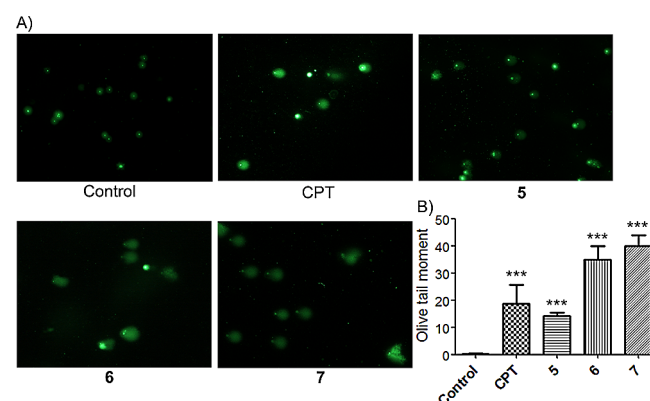


**Figure 3.** Comet assays in HeLa cells and olive tail moment analyses. A) Comet assays in HeLa cells in the presence of compounds 5–7 and CPT at 10 μM. B) Olive tail moment of each compound. Ten comets chosen randomly from six different pictures were calculated by software and treated statistically; \*\*\**p* < 0.001 relative to untreated control.

## Molecular docking studies

In an attempt to understand the molecular basis for topo I inhibition, molecular docking analyses were performed to predict the binding modes of representative compound **6** (*R* and *S* isomers) with topo I by using the C-DOCKER program within the Discovery Studio 2.1 software package. The published X-ray crystal structure of the topo I–DNA–topotecan complex (PDB ID: 1K4T) was used for docking calculations.

Similar binding modes of (*R*)- and (*S*)-**6** with the topo I–DNA cleavage complex were obtained in the docking studies (Figure 4). Like CPT and topotecan, (*R*)- and (*S*)-**6** were also

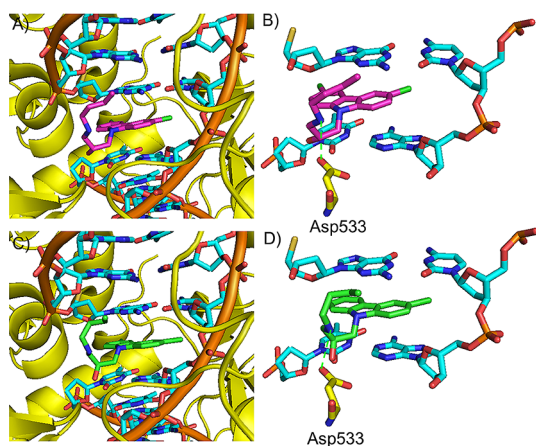


**Figure 4.** Molecular docking analysis of (*R*)- and (*S*)-**6** with the topo I–DNA cleavage complex. A) 3D schematic interaction model of (*R*)-**6** (magenta) and the topo I–DNA complex; B) binding mode of (*R*)-**6** with contacting residues and base pairs of the topo I–DNA complex; C) 3D schematic interaction model of (*S*)-**6** (green) and the topo I–DNA complex; D) binding mode of (*S*)-**6** with contacting residues and base pairs of the topo I–DNA complex. Hydrogen bonds are highlighted as green dashes.

found to intercalate into DNA at the DNA cleavage site and to form base-stacking interactions with downstream (–1) T:A and upstream (+1) G:C base pairs (Figure 4A,C). In addition, both isomers formed one hydrogen bond with Asp533, a residue near the active site, which is known to be necessary for topo I sensitivity to CPT.<sup>[4]</sup> The hydrogen bond occurs between the nitrogen atom of the amine tail of **6** (donor) and carboxylate ion of Asp533 (acceptor, Figure 4B,D). The predicted binding modes are consistent with our experimental data, indicating that compound **6** stabilizes the topo I–DNA cleavage complex like CPT, and probably acts as a topo I poison.

## Induction of cell-cycle arrest and apoptosis

As illustrated above, the representative derivatives **5–7** could effectively inhibit topo I, induce DNA damage, and inhibit the proliferation of multiple cancer cell lines. Thus, the most potent compound **6** was selected for further studies of its effect on cell-cycle progression and the induction of apoptosis in HeLa cells.

| Sample            | Phase                  |                    |       |                    |
|-------------------|------------------------|--------------------|-------|--------------------|
|                   | Sub-G <sub>1</sub> [%] | G <sub>1</sub> [%] | S [%] | G <sub>2</sub> [%] |
| Control           | 5.34                   | 45.27              | 29.01 | 12.50              |
| <b>6</b> (0.5 μM) | 8.87                   | 42.38              | 28.63 | 13.90              |
| <b>6</b> (1 μM)   | 6.37                   | 49.67              | 23.84 | 16.06              |
| <b>6</b> (5 μM)   | 12.93                  | 47.16              | 17.68 | 18.33              |
| <b>6</b> (10 μM)  | 49.41                  | 29.16              | 13.24 | 8.25               |

As summarized in Table 2, a dose-dependent increase in G<sub>2</sub> and sub-G<sub>1</sub> populations was observed in response to the treatment by compound **6**. G<sub>2</sub>-phase arrest usually occurs in response to DNA damage, preventing the transmission of damage to daughter cells.<sup>[21]</sup> The percentage of cells in G<sub>2</sub> and sub-G<sub>1</sub> phases increased remarkably after treatment with compound **6** at 5 μM, from 12.5 to 18.3% and 5.3 to 12.9%, respectively. At a concentration of 10 μM compound **6**, around half of the cells entered the sub-G<sub>1</sub> phase (apoptosis). The results indicate that **6** induces G<sub>2</sub>-phase cell-cycle arrest followed by apoptosis in HeLa cells.

Consistent with the dramatically increased sub-G<sub>1</sub> cell population occurring in cell-cycle analysis, a dose-dependent increase in the percentage of apoptotic and dead cells was also observed in the apoptosis assay (Figure 5). Annexin V-FITC analysis revealed a basal apoptotic population of 6.1% in the untreated culture. After incubation for 24 h, compound **6** (20 μM) induced almost all of the HeLa cells into the apoptotic stage (43.9% in late stage and 55.2% in early stage). Thus, apoptosis is the primary mode of cell death induced by **6**.

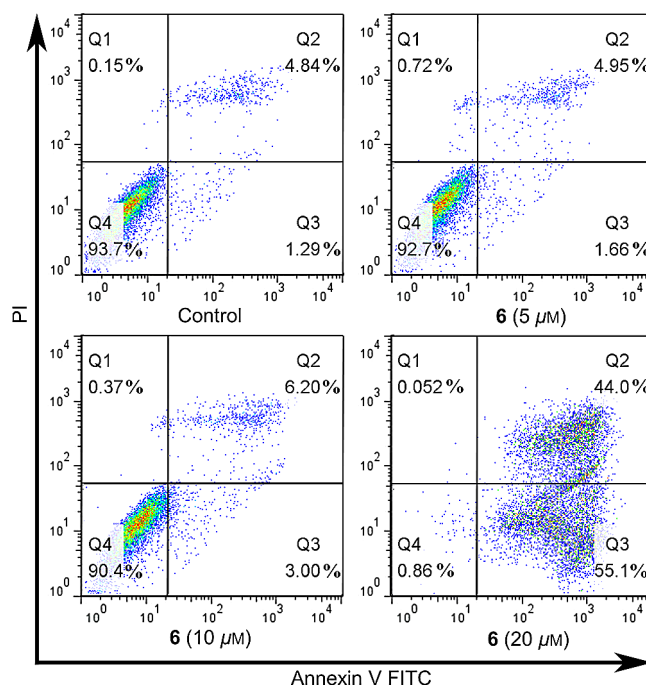


**Figure 5.** Apoptotic cells were detected by Annexin V/PI double staining after incubation with compound **6** (5, 10, and 20 μM) for 24 h.

## Conclusions

In this study, carbazole aminoalcohol derivatives were synthesized and evaluated as a series of novel antitumor agents. SAR studies revealed that the aliphatic-amine-substituted derivatives are more potent antitumor agents than those with aromatic amino groups. Among them, alkylamine-substituted compounds **5–7** exhibited the most efficient antiproliferative activity, which is in accordance with their topo I inhibitory ability. Through comet assays and molecular docking analyses, we speculate that the representative compounds **5–7** act as topo I poisons, which cause single-strand DNA damage by stabilizing the topo I–DNA cleavage complex. Furthermore, the most potent compound **6** induced G<sub>2</sub>-phase arrest and apoptosis in HeLa cells. This study identified the antitumor activity of a series of carbazole aminoalcohols and discovered a novel topo I inhibitor scaffold, which may be promising for the development of new anticancer agents.

## Experimental Section

### Chemistry

Reagents and solvents were purchased from Sigma–Aldrich and were used without further purification. Melting points were determined with a B-540 Büchi apparatus and are uncorrected. <sup>1</sup>H and <sup>13</sup>C NMR spectra were recorded on a Bruker AM-400 spectrometer (400 MHz). Chemical shifts ( $\delta$ ) are given in ppm relative to TMS as internal standard, and signals are denoted with the following abbreviations: s, singlet; d, doublet; t, triplet; m, multiplet. Mass spectra (MS, ESI) were recorded on a Thermo Q Exactive Orbitrap LC–MS/MS instrument. Thin-layer chromatography (TLC) was carried out using plate silica gel F<sub>254</sub> (Merck). All yields are unoptimized and generally represent the result of a single experiment. Elemental analyses (C, H, and N) were undertaken using an Elementar Vario ELIII analyzer. Analytical HPLC was performed on a Waters 2695-2996 HPLC system and an Elite hypersil BDS C<sub>18</sub> column (5  $\mu$ m, 4.6  $\times$  250 mm) using the following binary solvent system: CH<sub>3</sub>CN/0.1% aqueous trifluoroacetic acid (TFA) = 85:15; flow rate: 1.0 mL min<sup>-1</sup>,  $\lambda$  = 254 nm, column temperature = 30 °C. The purities of all test compounds determined by HPLC were > 95%.

**General procedures for the synthesis of 9-(oxiran-2-ylmethyl)-9H-carbazoles (2a–c):** To a cooled solution of compounds **1a–c** (2 mmol) in DMF (20 mL, 0 °C), KOH (135 mg, 2.4 mmol) was added slowly. After stirring for an additional 1 h, epoxy chloropropane (2.4 mmol) was added dropwise. The progress of the reaction was monitored by TLC. The reaction was quenched with water (30 mL). The resulting mixture was extracted with ethyl acetate (3  $\times$  20 mL). Organic layer was washed with water (3  $\times$  50 mL) and brine (3  $\times$  50 mL), dried over anhydrous Na<sub>2</sub>SO<sub>4</sub>. The solvent was evaporated under reduced pressure and dried under high vacuum overnight. The solid was used directly in the epoxide opening reaction without further purification.

**General procedures for the synthesis of carbazole aminoalcohols (3–18):** To a solution of 9-(oxiran-2-ylmethyl)-9H-carbazole (**2a–c**, 2 mmol) in EtOH (20 mL), corresponding amines (6 mmol) was added. For low reactive amines (e.g., arylamines), BiCl<sub>3</sub> (1 mmol) was also added. The reaction mixture was heated at reflux for 6 h. The progress of the reaction was monitored by TLC. After reaction, the mixture was quenched with water (10 mL) and

extracted with EtOAc (3  $\times$  10 mL). The organic phase was washed with water (3  $\times$  20 mL) and brine (3  $\times$  20 mL), dried over anhydrous Na<sub>2</sub>SO<sub>4</sub>, and concentrated under reduced pressure. The obtained residues were purified by recrystallization from ethanol to afford target compounds **3–18**. The structural characterization of target compounds is described in the Supporting Information.

**1-(3,6-Dichloro-9H-carbazol-9-yl)-3-(piperidin-1-yl)propan-2-ol (3):** white solid (66%, over two steps), mp: 140.3–141.3 °C.

**1-(3,6-Dichloro-9H-carbazol-9-yl)-3-(2-methylpiperidin-1-yl)propan-2-ol (4):** white solid (70%, over two steps), mp: 131.8–133.4 °C.

**1-(3,6-Dichloro-9H-carbazol-9-yl)-3-(propylamino)propan-2-ol (5):** white solid (71%, over two steps), mp: 117.6–120.1 °C.

**1-(Butylamino)-3-(3,6-dichloro-9H-carbazol-9-yl)propan-2-ol (6):** white solid (50%, over two steps), mp: 116.9–118.1 °C.

**1-(3,6-Dichloro-9H-carbazol-9-yl)-3-(pentylamino)propan-2-ol (7):** white solid (59%, over two steps), mp: 98.5–99.6 °C.

**1-(3,6-Dichloro-9H-carbazol-9-yl)-3-(phenylamino)propan-2-ol (8):** white solid (59%, over two steps), mp: 140.3–142.0 °C.

**1-(3,6-Dichloro-9H-carbazol-9-yl)-3-((4-fluorophenyl)amino)propan-2-ol (9):** white solid (53%, over two steps), mp: 137.7–140.3 °C.

**1-((4-Bromophenyl)amino)-3-(3,6-dichloro-9H-carbazol-9-yl)propan-2-ol (10):** white solid (43%, over two steps), mp: 154.8–157.4 °C.

**1-((4-Chlorophenyl)amino)-3-(3,6-dichloro-9H-carbazol-9-yl)propan-2-ol (11):** white solid (71%, over two steps), mp: 139.6–143.0 °C.

**1-(3,6-Dichloro-9H-carbazol-9-yl)-3-(p-tolylamino)propan-2-ol (12):** white solid (66%, over two steps), mp: 157.9–160.5 °C.

**1-(3,6-Dichloro-9H-carbazol-9-yl)-3-(o-tolylamino)propan-2-ol (13):** white solid (69%, over two steps), mp: 108.7–111.6 °C.

**1-(3,6-Dichloro-9H-carbazol-9-yl)-3-((4-methoxyphenyl)amino)propan-2-ol (14):** white solid (63%, over two steps), mp: 164.6–167.4 °C.

**1-(Benzylamino)-3-(3,6-dichloro-9H-carbazol-9-yl)propan-2-ol (15):** white solid (68%, over two steps), mp: 139.8–142.5 °C.

**1-(3,6-Dichloro-9H-carbazol-9-yl)-3-((3,4-dimethoxyphenethyl)amino)propan-2-ol (16):** white solid (61%, over two steps), mp: 138.5–139.4 °C.

**1-(Butylamino)-3-(9H-carbazol-9-yl)propan-2-ol (17):** white solid (58%, over two steps), mp: 114.2–115.1 °C.

**1-(Butylamino)-3-(3,6-dibromo-9H-carbazol-9-yl)propan-2-ol (18):** white solid (53%, over two steps), mp: 123.4–124.8 °C.

### Biological evaluation

**Cell culture:** HeLa and HL60 cell lines were obtained from Shanghai Institute of Materia Medica, Chinese Academy of Sciences. HeLa cells were cultured in adherence in MEM (Gibco, USA) containing 10% fetal bovine serum (Lanzhou Lark, China), 1% sodium pyruvate (Sigma, USA) and 1% GlutaMAX-I (Gibco, USA). HL60 cells were cultivated in suspension in RPMI-1640 (HyClone, USA) containing 10% fetal bovine serum. Cultures were performed in a hu-

modified incubator (Thermo, USA) in an atmosphere of 5% CO<sub>2</sub> at 37 °C.

**Cytotoxicity assay:** Sulforhodamine B (SRB) and MTT assays were performed on adherent and suspended cells, respectively. HeLa and HL60 cells were planted into 96-well plates at a densities of 3000 and 6000 cells per well, respectively. After incubation for 24 h, cells were treated with compounds at gradient concentrations for 72 h. For the SRB assay, cells were fixed with 10% trichloroacetic acid, and then stained with SRB (TCI, Japan). Free dye was washed by 1% acetic acid solution. Conjugate SRB was dissolved by 10 mM Tris solution. Plates were measured at  $\lambda = 560$  nm on a Synergy 2 Multi-Mode Reader (BioTek, USA). For MTT assays, 20  $\mu$ L of 5 mg mL<sup>-1</sup> MTT (Amresco, USA) solution was added to each well and incubated for 4 h to form formazan. Formazan was incubated by Lysis solution (10% SDS, 5% isobutyl alcohol, 0.012 mM HCl) overnight. Plates were examined at  $\lambda = 570$  nm. The inhibition rate was calculated by the following formula [Eq. (1)]:

$$\text{Inhibition rate} = \left( 1 - \frac{\text{OD}_{\text{treated}} - \text{OD}_{\text{blank}}}{\text{OD}_{\text{control}} - \text{OD}_{\text{blank}}} \right) \times 100\% \quad (1)$$

IC<sub>50</sub> values were then calculated.

**Topo I-mediated DNA relaxation assay:** The topo I inhibitory action of compounds was tested by relaxing supercoiled pBR322 DNA. DNA topoisomerase I assay kit and pBR322 DNA were purchased from TAKARA. 0.05  $\mu$ g pBR322 DNA, 0.05 U topoisomerase I, 2  $\mu$ L 0.1% BSA, and indicated concentrations of compounds were added in diluted assay buffer to a volume of 20  $\mu$ L, and incubated for 30 min at 37 °C. The reaction was started by adding topoisomerase I, and stopped by 2  $\mu$ L 10% SDS and 2  $\mu$ L DNA loading buffer (TianGen, China). Samples were electrophoresed in 1% agarose gel in TAE buffer for 2 h at 50 V. Gel was stained with 5  $\mu$ g mL<sup>-1</sup> ethidium bromide for 10 min, and photographed at 254 nm UV.

**Comet assay:** Single-strand DNA damage was evaluated by comet assay. HeLa cells were seeded in a six-well plate at a density of  $2 \times 10^5$  cells per well. After incubation for 24 h, cells were treated with indicated concentrations of compounds for 24 h, and collected and washed three times with D-Hanks solution. The cell density was adjusted to  $10^5$  cells per mL; 5  $\mu$ L of cells were mixed with 75  $\mu$ L of 0.5% low-melting-point agarose (Amresco, USA) which was prepared and sub-packaged previously and was melted and kept warm at 37 °C before the experiment. The mixture was spread on a 1% NMA coated slide with a coverslip and solidified on ice. The coverslip was removed and the slide was immersed into cold fresh lysis solution (2.5 M NaCl, 100 mM EDTA, 10 mM Tris, 1% Triton X-100, 10% DMSO) for 2 h at 4 °C in the dark. The slide was removed from the lysis solution and washed in Tris solution for 5 min three times, and then unwinding DNA in electrophoresis buffer (300 mM NaOH, 1 mM EDTA, pH > 13, made freshly) for 30 min at 4 °C in the dark. The slide was electrophoresed for 25 min at 15 V at 4 °C in the dark. The slide was neutralized with Tris-HCl buffer (0.4 M Tris, pH 7.5) for 5 min three times, and dried with anhydrous ethyl alcohol. The slide was stained with SYBR Green I (Life, USA) before observation, and photographed under blue light with a Ti-S Fluorescence microscope (Nikon, Japan). Olive tail moment was statistically treated with CASP (Comet Assay Software Project).

**Computational methods:** Docking simulations were carried out with the CDocker module (Discovery Studio, version 2.1, Accelrys, San Diego, CA, USA). The X-ray crystal structure of the topoisomer-

ase I-DNA-topotecan complex (PDB ID: 1K4T) was used for the docking calculation. After removing the ligand and solvent molecules, the CHARMM force field was applied to the protein, and the area around intercalation sites was chosen as the active site with a radius set as 9 Å. At physiologically relevant pH (7.4), both nitrogen atoms of **6** are protonated (see Figure S1 in the Supporting Information). Accordingly, they were charged at +1 for docking simulations. Each isomer of **6** was generated random conformations using CHARMM-based molecular dynamics (1000 steps), and then docked into the defined binding site. The other parameters were set as default. The final binding conformations of (*R*)- and (*S*)-**6** were determined based on the calculated CDocking energy and visual check. The most stable binding mode among the top 10 docking poses of each isomer is presented in Figure 4.

**Cell-cycle analysis by flow cytometry:** Cell-cycle analysis was performed with PI/RNase solution purchased from Sungene. HeLa cells were planted into a six-well plate at a density of  $2 \times 10^5$  cells per well. Cells were treated with compounds for 24 h and then harvested. After washing with D-Hanks solution twice, cells were fixed with 70% ethyl alcohol at 4 °C overnight. The next day, samples were washed and stained with PI/RNase solution for 30 min at room temperature. Samples were then analyzed on a flow cytometer (BD Biosciences, USA). And data were treated with FlowJo.

**Apoptosis analysis by flow cytometry:** Annexin V-FITC Cell Apoptosis Analysis Kit was purchased from Sungene. After the same treatment on HeLa cells (see cell-cycle analysis), cells were collected and washed three times with D-Hanks and then washed with binding buffer. Samples were stained with Annexin V-FITC solution and PI solution. Samples were analyzed by flow cytometry.

**Statistical analysis:** Data are expressed as the mean  $\pm$  SD unless otherwise indicated. Statistical analysis of data for multiple groups was performed with one-way analysis of variance (ANOVA). Student's *t*-test was applied for the comparison of two groups, and *p* values < 0.01 are considered significant.

## Acknowledgements

This work was supported financially by the Fundamental Research Funds for the Central Universities (China), the National Natural Science Foundation of China (Grant Nos. 21302054 and 21502181; Z.C. and W.W.), the Shanghai Committee of Science and Technology (Grant No. 13ZR1453100; Z.C.), and the Opening Fund of Shanghai Key Laboratory of Chemical Biology (Grant No. SKLCB-2012-05; Z.C.).

**Keywords:** antitumor agents · apoptosis · carbazole aminoalcohols · cell-cycle arrest · topoisomerase I

- [1] J. J. Champoux, R. Dulbecco, *Proc. Natl. Acad. Sci. USA* **1972**, *69*, 143–146.
- [2] S. H. Chen, N. L. Chan, T. S. Hsieh, *Annu. Rev. Biochem.* **2013**, *82*, 139–170.
- [3] J. J. Champoux, *Annu. Rev. Biochem.* **2001**, *70*, 369–413.
- [4] B. L. Staker, K. Hjerrild, M. D. Feese, C. A. Behnke, A. J. Burgin, L. Stewart, *Proc. Natl. Acad. Sci. USA* **2002**, *99*, 15387–15392.
- [5] M. E. Wall, M. C. Wani, C. E. Cook, K. H. Palmer, A. T. Mcphail, G. A. Sim, *J. Am. Chem. Soc.* **1966**, *88*, 3888–3890.
- [6] Y. Pommier, *Nat. Rev. Cancer* **2006**, *6*, 789–802.
- [7] Y. Pommier, *Acs Chem. Biol.* **2013**, *8*, 82–95.

- [8] J. Janočková, J. Plšíková, J. Kašpárková, V. Brabec, R. Jendželovský, J. Mikeš, J. Koval, S. Hamuláková, P. Fedoročko, K. Kuča, M. Kožurková, *Eur. J. Pharm. Sci.* **2015**, *76*, 192–202.
- [9] H. B. Kwon, C. Park, K. H. Jeon, E. Lee, S. E. Park, K. Y. Jun, T. M. Kadayat, P. Thapa, R. Karki, Y. Na, M. S. Park, S. B. Rho, E. S. Lee, Y. Kwon, *J. Med. Chem.* **2015**, *58*, 1100–1122.
- [10] T. M. Kadayat, C. Song, S. Shin, T. B. Magar, G. Bist, A. Shrestha, P. Thapa, Y. Na, Y. Kwon, E. S. Lee, *Bioorg. Med. Chem.* **2015**, *23*, 3499–3512.
- [11] T. Sripisut, S. Laphookhieo, *J. Asian Nat. Prod. Res.* **2010**, *12*, 614–617.
- [12] A. W. Schmidt, K. R. Reddy, H. J. Knolker, *Chem. Rev.* **2012**, *112*, 3193–3328.
- [13] A. Gluszyńska, *Eur. J. Med. Chem.* **2015**, *94*, 405–426.
- [14] F. C. Huang, C. C. Chang, J. M. Wang, T. C. Chang, J. J. Lin, *Br. J. Pharmacol.* **2012**, *167*, 393–406.
- [15] R. Akué-Gedu, B. Letribot, E. Saugues, E. Debiton, F. Anizon, P. Moreau, *Bioorg. Med. Chem. Lett.* **2012**, *22*, 3807–3809.
- [16] K. Kinoshita, K. Asoh, N. Furuichi, T. Ito, H. Kawada, S. Hara, J. Ohwada, T. Miyagi, T. Kobayashi, K. Takanashi, T. Tsukaguchi, H. Sakamoto, T. Tsukuda, N. Oikawa, *Bioorg. Med. Chem.* **2012**, *20*, 1271–1280.
- [17] C. Sherer, T. J. Snape, *Eur. J. Med. Chem.* **2015**, *97*, 552–560.
- [18] J. Molette, J. Routier, N. Abla, D. Besson, A. Bombrun, R. Brun, H. Burt, K. Georgi, M. Kaiser, S. Nwaka, M. Muzerelle, A. Scheer, *ACS Med. Chem. Lett.* **2013**, *4*, 1037–1041.
- [19] S. Bertini, V. Asso, E. Ghilardi, C. Granchi, C. Manera, F. Minutolo, G. Saccomanni, A. Bortolato, J. Mason, S. Moro, M. Macchia, *Bioorg. Med. Chem. Lett.* **2011**, *21*, 6657–6661.
- [20] M. Herrera, G. Dominguez, J. M. Garcia, C. Pena, C. Jimenez, J. Silva, V. Garcia, I. Gomez, R. Diaz, P. Martin, F. Bonilla, *Clin. Cancer Res.* **2009**, *15*, 5466–5472.
- [21] T. Chen, P. A. Stephens, F. K. Middleton, N. J. Curtin, *Drug Discovery Today* **2012**, *17*, 194–202.

---

Manuscript received: August 3, 2016

Revised: October 24, 2016

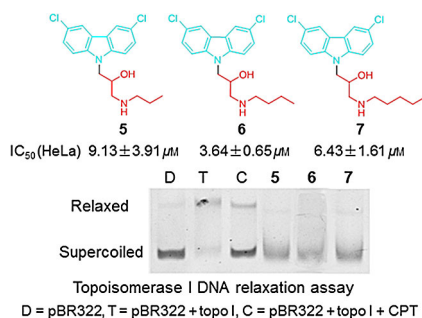
Final Article published: ■ ■ ■, 0000

## FULL PAPERS

W. Wang, X. Sun, D. Sun, S. Li, Y. Yu,  
T. Yang, J. Yao, Z. Chen,\* L. Duan\*



### Carbazole Aminoalcohols Induce Antiproliferation and Apoptosis of Human Tumor Cells by Inhibiting Topoisomerase I



**Under arrest:** Carbazole aminoalcohols were synthesized and tested for their inhibitory potential against topoisomerase I (topo 1) and for their antiproliferative activity against human tumor cell lines. Structure–activity relationships indicated that alkylamine-substituted compounds exhibit the most efficient antiproliferative activity, in agreement with their topo I inhibitory capacity. Further studies confirmed that the most potent compound induces G<sub>2</sub>-phase cell-cycle arrest and apoptosis in HeLa cells.